Macfarlane, D. E., & Mills, D. C. B. (1981) *J. Cyclic Nucleotide Res. 7*, 1–11.
Macfarlane, D. E., Wright, B. S., & Stump, D. C. (1981) *Thromb. Res. 24*, 31–43.
Mellwig, K. P., & Jakobs, K. H. (1980) *Thromb. Res. 18*, 7–17.
Mills, D. C. B., & Smith, J. B. (1971) *Biochem. J. 121*, 185–196.
Mills, D. C. B., & Smith, J. B. (1972) *Ann. N.Y. Acad. Sci. 201*, 391–399.
Mills, D. C. B., & Macfarlane, D. E. (1976) in *Platelets in Biology and Pathology* (Gordon, J. L., Ed.) pp 159–202, Elsevier, Amsterdam.
Mills, D. C. B. & Macfarlane, D. E. (1977) *Thromb. Haemostasis 38*, 82.
Nachman, R. L. (1975) *Ciba Found. Symp., New Ser. 35*, 23–46.
Nachman, R. L. & Ferris, B. (1974) *J. Biol. Chem. 249*, 704–710.
Neville, D. M. (1971) *J. Biol. Chem. 246*, 6328–6334.
Newman, K. C., Williams, L. T., Bishoprick, N. H., & Lefkowitz, R. J. (1978) *J. Clin. Invest. 61*, 395–402.
Pearce, P. H., & Scrutton, M. C. (1977) *Thromb. Haemostasis 38*, 82.
Robey, F. A., Jamieson, G. A., & Hunt, J. B. (1979) *J. Biol. Chem. 254*, 1114–1118.
Schaeffer, J. H., & Thomas, J. H. (1958) *J. Am. Chem. Soc. 80*, 3738–3742.
Siegl, A. M., Smith, J. B., Silver, M. J., Nicolaou, K. C., & Ahern, D. (1979a) *J. Clin. Invest. 63*, 215–220.
Siegl, A. M., Smith, J. B., Silver, M. J. (1979b) *Biochem. Biophys. Res. Commun. 90*, 291–296.
Sowa, T., & Ouchi, S. (1975) *Bull. Chem. Soc. Jpn. 48*, 2084–2090.
Steer, M. L., & Wood, A. (1979) *J. Biol. Chem. 254*, 10791–10797.
Tateson, J. E., Moncada, S., & Vane, J. R. (1977) *Prostaglandins 13*, 389–397.
Temple, C., Kussner, C. L., & Montgomery, J. A. (1966) *J. Org. Chem. 31*, 935–938.
Walsh, P. N., Mills, D. C. B., & White, J. G. (1977) *Br. J. Haematol. 36*, 281–296.

Binding of Calcium and Magnesium to Myosin in Skeletal Muscle Myofibrils†

Julian Borejdo*,‡ and Moshe M. Werber

ABSTRACT: Binding profiles for divalent cation to myosin have been obtained in myofibrils where myosin is assembled in arrays typical of the in vivo organization. Protection by Ca^{2+} and Mg^{2+} ions of the regions of myosin susceptible to chymotryptic attack provided the means to monitor metal ion binding. The effect of various concentrations of divalent cations on the chymotryptic digestion patterns was assessed by densitometry of Coomassie Blue stained gels obtained by polyacrylamide gel electrophoresis in the presence of sodium dodecyl sulfate and by the rate of myofibrillar solubilization. The results indicate the presence of two classes of binding sites differing in affinity by 4 orders of magnitude. The fractional saturation of the high-affinity site associated with the 5,5′-dithiobis(2-nitrobenzoic acid)-dissociable light chains of myosin regulated the production of subfragment 1 of myosin. From the digestion profiles as a function of metal ion concentration, binding constants for Mg^{2+} and Ca^{2+} were obtained. The value for Mg^{2+} was 5.7×10^6 M^{-1}, which is about 1 order of magnitude higher than the most recently determined values for free myosin in solution; the value for Ca^{2+} was 6.3×10^6 M^{-1}. Binding to the low-affinity site regulated the production of the heavy meromyosin fragment and yielded association constants for Ca^{2+} and Mg^{2+} of 0.9×10^3 and 0.7×10^3 M^{-1}, respectively.

It is well-known that skeletal myosin has two protease-sensitive regions. Proteolysis of the first region leads to the formation of subfragment 1 (S-1)[1] of myosin and can be regulated in vitro by binding of divalent cations to the metal binding site associated with the Nbs_2-dissociable light chains (Nbs_2 light chains; Bálint et al., 1971). Saturation of these sites (two per mole of myosin) with either Ca^{2+} or Mg^{2+} inhibits formation of S-1 (Weeds & Pope, 1977). Proteolysis of the second protease-sensitive region of myosin leads to the formation of HMM. Until now, there were no reports suggesting that the rate of proteolysis at this site can be regulated by binding of divalent cations.

The protease-sensitive regions may play an essential part in the mechanism of muscle contraction (Huxley, 1969; Highsmith et al., 1977). However, it is not at all clear whether binding of divalent cations to these sites has any physiological relevance. In particular, it has been shown that binding of divalent cations to the Nbs_2 light chains does not affect the disposition or rotational mobility of myosin heads with respect to the thick filament backbone (Mendelson & Cheung, 1976; Sutoh & Harrington, 1977).

† From the Polymer Research Department, Weizmann Institute of Science, Rehovot 76 100, Israel (J.B.), and Medical Laboratories, Meir Hospital, Kfar Sava 44 281, Israel (M.M.W.). *Received July 6, 1981.* This work was supported by a grant from the U.S.-Israel Binational Science Foundation.
‡ Established Investigator of the American Heart Association.

[1] Abbreviations: $NaDodSO_4$, sodium dodecyl sulfate; HMM, heavy meromyosin; S-1, heavy meromyosin subfragment 1; S-2, heavy meromyosin subfragment 2; Nbs_2 light chain, 19 000 molecular weight subunit of myosin dissociated by treatment with 5,5′-dithiobis(2-nitrobenzoic acid); LMM, light meromyosin; EGTA, ethylene glycol bis(β-aminoethyl ether)-*N,N,N′,N′*-tetraacetic acid; EDTA, ethylenediaminetetraacetic acid; PMSF, phenylmethanesulfonyl fluoride; K_a, association constant; rms, root mean square; K_d, dissociation constant.

0006-2960/82/0421-0549$01.25/0

Several studies, on the other hand, reveal striking effects of divalent cations on myosin. Thus, binding of divalent cations prevents chymotryptic attack at the S-1 site (Weeds & Pope, 1977), and in molluscan muscle, actin-activated MgATPase is modulated by binding of Ca^{2+} ions to a light chain homologous to the Nbs_2 chain, the so-called regulatory light chain. In many other muscles too, Ca^{2+} is able to regulate ATPase activity [see Lehman & Szent-Györgyi (1975) for a review]. Further, binding of Ca^{2+} and Mg^{2+} to the Nbs_2 light chains is affected by phosphorylation and accompanied by large conformational changes (Alexis & Gratzer, 1978; Kardami et al., 1980). For these reasons, a number of authors have studied the equilibrium binding of divalent cations either to isolated light chains (Werber et al., 1972; Morimoto & Harrington, 1974; Alexis & Gratzer, 1978) or to myosin and its proteolytic fragment HMM (Sugden & Nihei, 1969; Werber et al., 1973; Beinfeld et al., 1975; Morimoto & Harrington, 1974; Werber, 1978; Holroyde et al., 1979; Watterson et al., 1979; Kardami et al., 1980).

All the studies mentioned above have been carried out in solution and in the absence of actin. In muscle, however, myosin is arranged in a well-defined spatial configuration with fixed interfilament distances where entropic and/or dielectric constant effects on metal ion binding may be important. Such effects are in fact most likely responsible for the difference in affinity for calcium between the free and bound Nbs_2 light chains (Bagshaw, 1977; Bagshaw & Kendrick-Jones, 1979). Furthermore, in rigor myosin heads are bound to actin, and the Nbs_2 light chain conformation and/or environment may thus be affected. In fact, it has recently been suggested that actin does partially protect Nbs_2 chains in situ from proteolysis (Oda et al., 1980).

In this paper, we have studied the metal binding properties of the myosin in vivo. Working at pH 8.5 made both the S-1 and HMM junctions accessible to chymotrypsin. We have employed two parallel methods for the assessment of the fractional occupancy of the binding sites. In the first method, we have measured, by densitometry of Coomassie Blue stained gels obtained by polyacrylamide gel electrophoresis in the presence of $NaDodSO_4$, the products of chymotryptic digestions. In the second method, we have followed the rate of solubilization of myofibrils which proved to be proportional to the rate of proteolysis. We find that the affinity of magnesium for the Nbs_2 light chain of myosin in vivo is greater than that reported for myosin in vitro. We also find an additional low-affinity metal binding site at the HMM/LMM junction.

Materials and Methods

α-Chymotrypsin was obtained from Worthington Biochemicals. PMSF was from Sigma. All other chemicals were of analytical grade.

Preparation of Myofibrils and Proteins. Myofibrils were prepared from glycerinated fibers of rabbit psoas muscle. A thin strip of fibers was first transferred from glycerinating solution which contained EGTA and ATP to a cold rigor solution containing 80 mM KCl, 5 mM sodium phosphate buffer, pH 7.0, and 2 mM EDTA in order to inhibit rigor contraction. After 30 min, the fibers were again transferred to a new rigor solution containing 80 mM KCl and 1 mM sodium phosphate buffer, pH 7.0. After 30 min, the fibers were homogenized in a Sorvall Omni mixer at 8 speed setting, for 18 s in ice. PMSF was not added to myofibrils although this caused progressive damage to the Z lines by the endogenous proteases over a period of several days. Myofibrils were gently centrifuged in order to remove the debris and resuspended in a solution containing 80 mM KCl and 20 mM Tris-HCl buffer, pH 8.5. They were used on the day of preparation. The myofibrillar concentrations were determined by the biuret method.

Solutions. Free metal ion concentrations were maintained by using metal ion–EDTA buffers. The absolute stability constants for Mg–EDTA, Ca–EDTA, and H^+–EDTA complexes were taken from Fabiato & Fabiato (1979). The equilibria considered were metal–EDTA and metal–light chain. Apparent association constants for metal–light chain binding were taken from Werber et al. (1972), but this equilibrium was unimportant because of the low myosin concentration used (see below). All computations were done on an Apple II microcomputer. All solutions contained appropriate concentrations of metal and EDTA in addition to 80 mM KCl–20 mM Tris-HCl buffer, pH 8.5.

Quantitative $NaDodSO_4$ Gel Electrophoresis. Polyacrylamide gel electrophoresis in the presence of $NaDodSO_4$ was carried out according to the procedure of Laemmli (1970) using a two-phase resolving gel (3% and 7.5% acrylamide). The protein distribution among the different bands of the Coomassie Brilliant Blue R stained gels was quantitated by scanning on a Beckman model CDS 200 densitometer. The absolute amounts of myosin, HMM, S-1, and actin were taken as the areas under the peaks corresponding to molecular weights of 200K, 150K + 130K, 90K, and 42K, respectively. The reported relative amounts of myosin, HMM, and S-1 were always normalized with respect to the amount of actin, which was found to be unaffected by proteolysis in agreement with Sutoh & Harrington (1977).

Chymotryptic Digestions. Digestions were carried out at room temperature in a solution containing 0.3 mg/mL myofibrillar protein in an appropriate buffer. The drop in turbidity was monitored in a Cary 118 spectrophotometer at 400 nm. For quantitation of the appearance of different myosin fragments by $NaDodSO_4$–polyacrylamide gel electrophoresis, 0.2 mL of 1.6 mg/mL myofibrils was digested with, unless otherwise stated, 10 μL of 2.5 mg/mL chymotrypsin. The reaction was stopped by adding 1 mM (final concentration) PMSF and 50 μL of the $NaDodSO_4$-containing buffer.

Data Analysis. The digestion profiles were fitted to a simple binding curve by a computer program which examined all possible combinations of K_a and B, where B was the saturating value of the measured variable. The K_a belonging to a pair of values giving the smallest rms deviation from the experimental data was chosen.

Optical Microscopy. The Zeiss Axiomat microscope with phase optics was used to obtain photomicrographs of myofibrils during proteolysis. The light source was a 100-W halogen lamp. A Zeiss Planapochromat 100×, N.A. = 1.3 objective was used throughout. Magnification of the image on the film was 320×. A built-in 35-mm camera with Kodak Plus X film (125 ASA) was used. Exposure time was about 1 s.

Results

All experiments reported below were carried out at pH 8.5 to ensure equal acess of the protease to both junctions (see Discussion).

We have used, in parallel, two methods of measuring the divalent cation binding profiles. In the first method (method I), we have digested myofibrils with chymotrypsin in the presence of increasing concentrations of free metal ions and determined the relative amounts of products by quantitative $NaDodSO_4$–polyacrylamide gel electrophoresis. The justification of this procedure for the case of the S-1 junction is that it is well established that there is only a single high-affinity

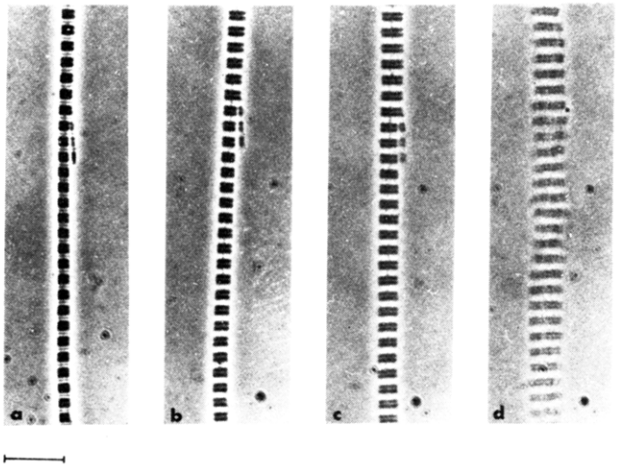

FIGURE 1: Photomicrographs of the time course of digestion of myofibrils. To myofibrils in 80 mM KCl–20 mM Tris-HCl buffer, pH 8.5, containing 0.02 μM free Mg^{2+} was added 125 μg/mL chymotrypsin at time 0. The photographs were taken at 10 s (a), 0.5 min (b), 3 min (c), and 7.5 min (d) after addition of chymotrypsin. The bar indicates 10 μm.

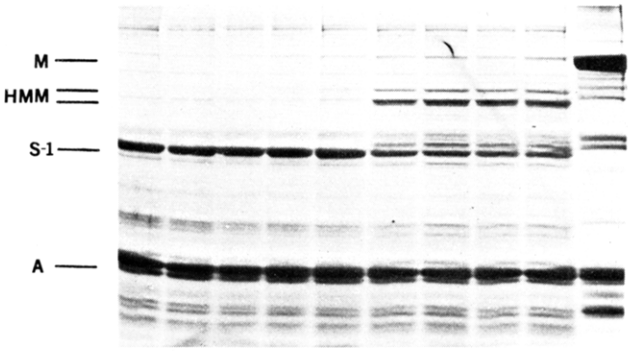

FIGURE 2: $NaDodSO_4$–polyacrylamide gel electrophoresis patterns of chymotryptic digests of myofibrils as a function of Mg^{2+} concentration. $NaDodSO_4$–polyacrylamide gel electrophoresis of digested myofibrils was run on composite 3 and 7.5% polyacrylamide gels. Myofibrils (1.6 mg/mL) were in 80 mM KCl–20 mM Tris-HCl buffer, pH 8.5. The concentration of free Mg was fixed by Mg–EDTA buffers with the constraint that $[Mg]_{bound}$ = 50 μM. Chymotrypsin (125 μg/mL) was added for 10 min, and the reaction was stopped by the addition of 1 mM PMSF. Free Mg^{2+} concentration was (from left to right, in micromolar) 0.01, 0.02, 0.03, 0.05, 0.1, 0.5, 1, 5, and 10. The first gel on the right is an intact myofibril. Positions of the heavy chains of myosin (M), HMM, S-1, and actin (A) are indicated at the left.

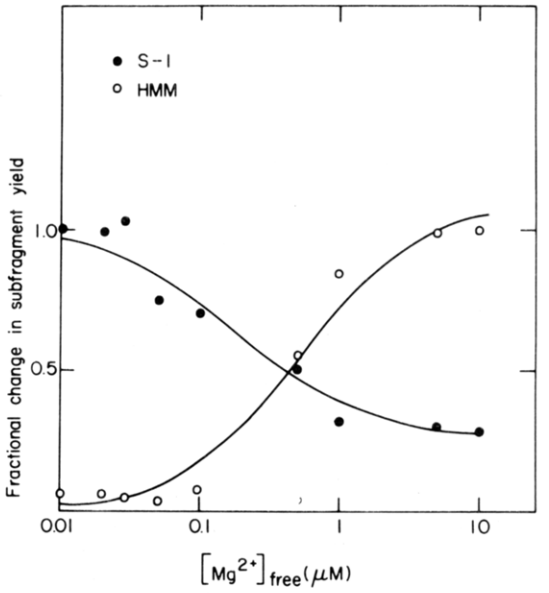

FIGURE 3: Chymotryptic digestion profiles for a high-affinity metal binding site of myosin in myofibrils (method I). Data from Figure 2. The amounts of S-1 (●) and HMM (○) produced at each Mg^{2+} concentration were quantitated by scanning the gels obtained by $NaDodSO_4$–polyacrylamide gel electrophoresis. The peaks corresponding to S-1 and HMM were normalized with respect to the amount of actin and expressed as the percentage of the amount of S-1 produced in the presence of 0.01 μM free Mg^{2+} (for S-1) and the amount of HMM produced in the presence of 10 μM Mg^{2+} (for HMM).

cation binding site on each myosin head (on the Nbs_2 light chain; Bagshaw, 1977) and that when occupied by either Ca^{2+} or Mg^{2+} S-1 is not formed (Weeds & Pope, 1977). The fractional change in S-1 production should therefore measure the fraction of binding sites occupied by the cation. By similar reasoning, it was assumed that the decrease in HMM production by increasing concentrations of Ca^{2+} or Mg^{2+} reflects the site occupancy by a cation near the HMM junction.

In the second method (method II), we have carried out the proteolysis while monitoring the drop in optical density of the myofibrillar suspension in the spectrophotometer. Production of the myosin fragments was expected to result in the solubilization of myofibrils as the thin filaments gradually become cut off from the thick filaments. Figure 1 shows the main features of the time course of the myofibrillar digestion (at any Mg^{2+} concentration). Following application of chymotrypsin, there was a rapid digestion of the Z lines accompanied by the digestion of the M-line material. The sensitivity of these myofibrillar components of proteolytic attack has been noted previously (Stromer et al., 1967; Garamvölgyi, 1968). After these components have been digested away, the only links holding the myofibril together are cross-bridges (Borejdo & Oplatka, 1981). When the cross-bridge is cleaved (either at the S-1 or at the HMM junction), the myofibril solubilizes. The rate of this process, visible in Figure 1 as a gradual swelling and solubilization, is expected to depend on the divalent cation concentration. We have found that the main product of digestion was HMM (high divalent metal ion concentration; see below), the rate of myofibrillar solubilization equalled the rate of HMM production. At low Mg^{2+} concentrations, the rate of solubilization equalled the rate of myosin digestion. The chief advantages of this method are that it is much less time consuming and more reproducible than the quantitative $NaDodSO_4$ gel analysis.

High-Affinity Site Binding Profiles. Figure 2 shows the in vivo titration of the Nbs_2 light chains with Mg^{2+}. Myofibrils were digested with chymotrypsin in the presence of increasing concentrations of free Mg^{2+} in the range 0.01 μM $\leq [Mg^{2+}]_{free} \leq$ 10 μM. The total concentrations of Mg^{2+} and EDTA required to obtain the desired free Mg^{2+} concentration were computed by fixing $[Mg]_{bound}$ = [Mg–EDTA] at 50 μM. This was much higher than the Mg^{2+} contamination in our water, estimated by atomic absorption to be between 0.5 and 1.2 μM, and higher than the total concentration of other metal binding proteins (maximum ca. 7.0 μM actin and ca. 1 μM troponin C). The main digestion product at low Mg^{2+} concentrations was S-1 and at higher Mg^{2+} concentrations HMM as well as S-1. Titrations with Ca^{2+} gave rise to a similar picture. The digestion profile of myosin obtained from the densitometric scan of the different gels in Figure 2 is shown in Figure 3. The association constant for the Mg^{2+} binding for the case of a single class of sites per myosin head was determined from the midpoint of the S-1 titration curve after subtracting the residual S-1 present at saturating Mg^{2+} concentration (Table I).

Table I: Association Constants for Ca^{2+} and Mg^{2+} Binding to High- and Low-Affinity Sites by Two Methods[a]

	K_a (M^{-1})			
	high affinity		low affinity	
metal	I[b]	II[c]	I	II
Ca^{2+}	6.3×10^6 [d]	4.1×10^7	0.9×10^3	1.8×10^3
Mg^{2+}	5.7×10^6	3.7×10^7	0.7×10^3	1.7×10^3

[a] The digestions were carried out at room temperature in 80 mM KCl–20 mM Tris-HCl, pH 8.5. [b] Method I, quantitative $NaDodSO_4$–polyacrylamide gel electrophoresis. [c] Method II, the rate of turbidity change. [d] Calculated from the value measured by method II, multiplied by the ratio of the values for the two methods in the case of Mg^{2+}.

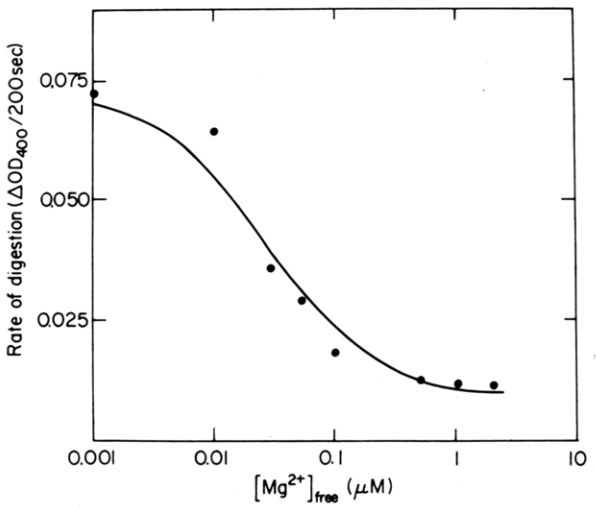

FIGURE 4: Chymotryptic digestion profiles for a high-affinity metal binding site of myosin in myofibrils (method II). The rate of digestion was assessed by measuring the rate of solubilization of myofibrils. Myofibrils were in 80 mM KCl–20 mM Tris-HCl, pH 8.5.

The high-affinity metal binding profiles were also obtained by method II. The time course of myofibrillar solubilization at a series of Mg^{2+} concentrations was followed after application of chymotrypsin. After the enzyme was added, there was an initial rapid phase of turbidity drop probably reflecting the digestion of the Z and M lines. This was followed by a slower, nearly linear phase which reflected the rate of myosin digestion, and which depended on the free divalent cation concentration. In Figure 4, the Mg^{2+} binding profile has been constructed by plotting the rate of digestion vs. the free Mg^{2+} concentration. High divalent cation concentrations ($\sim$10 μM) did not inhibit completely the digestion, because HMM formation was not affected by this metal ion concentration (see below). The affinity constants for Mg^{2+} and Ca^{2+} binding were determined from the midpoints of transitions after subtracting this residual rate and are listed in Table I.

Low-Affinity Site Binding Profiles. When the free divalent metal concentration is raised above 10 μM, the presence of the second metal binding site becomes apparent. Figure 5 shows the $NaDodSO_4$–polyacrylamide gel electrophoresis gels illustrating the titration of myofibrils with Ca^{2+} in the range from 50 μM to 20 mM. The titration curve for this effect obtained by scanning the $NaDodSO_4$–polyacrylamide gels is shown in Figure 6. Above about 100 μM Ca^{2+}, the amount of HMM produced begins to decline while the amount of undigested myosin begins to rise. A 2 mM concentration of Ca^{2+} was necessary to decrease the production of HMM to half of the amount produced below 50 μM Ca^{2+}. It was not possible to completely abolish the appearance of the 150K and 130K dalton bands even at 20 mM[2] free Ca^{2+} (Figure 7) (see

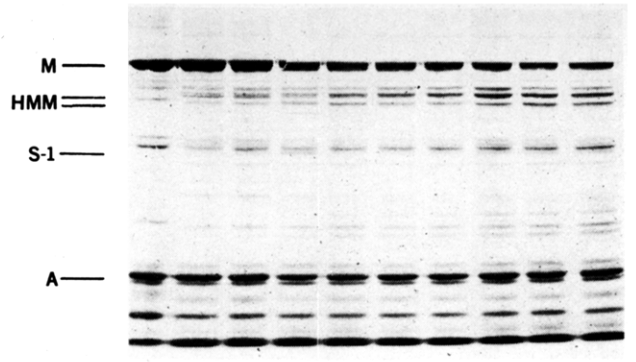

FIGURE 5: $NaDodSO_4$–polyacrylamide gel electrophoresis pattern of chymotryptic digest of myofibrils vs. Ca^{2+} concentration. $NaDodSO_4$–polyacrylamide gel electrophoresis was on 7.5% polyacrylamide. Myofibrils (1.6 mg/mL) in 80 mM KCl–20 mM Tris-HCl, pH 8.5, were digested with 125 μg/mL chymotrypsin for 10 min at room temperature. Ca^{2+} concentration was (from right to left) 50 μM, 100 μM, 200 μM, 500 μM, 1 mM, 2 mM, 5 mM, 10 mM, and 20 mM. The first gel on the left is an intact myofibril. The positions of the heavy chains of myosin (M), HMM, S-1, and actin (A) are indicated at the left.

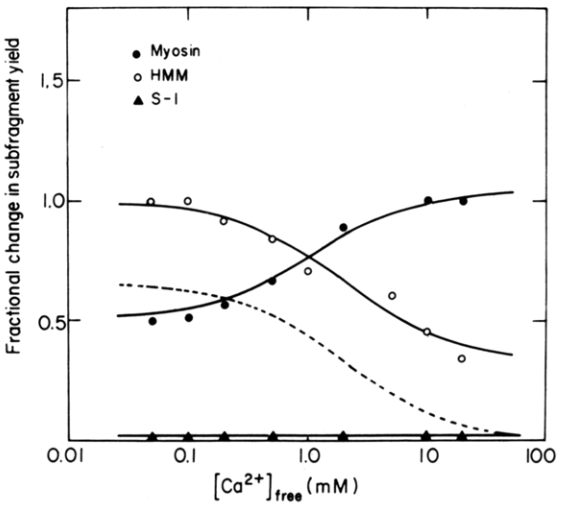

FIGURE 6: Chymotryptic digestion profile at the low-affinity site of myosin in myofibrils (method I). The amounts of S-1 (▲), heavy chains of HMM (○), and heavy chains of myosin (●) were quantitated by $NaDodSO_4$–polyacrylamide gel electrophoresis, normalized with respect to actin, and expressed as percentages of the amounts produced at 0.01 μM Ca^{2+} (for S-1) at 50 μM Ca^{2+} (for HMM) and in undigested myofibrils (for myosin). The broken line represents the digestion profile for HMM, assuming production of HMM is completely inhibited. See text for details.

Discussion). The association constants for Ca^{2+} and Mg^{2+} binding at the low-affinity site are given in Table I.

Another estimate of the binding constant is obtained by following the rate of absorbance change (method II). This rate was a measure of the rate of HMM formation (see Results). This is consistent with the fact that above 50 μM Ca^{2+} no significant amount of S-1 was produced (Figure 5) and that production of HMM was paralleled by the digestion of myosin (Figure 7). A typical Ca^{2+} binding profile determined by this method is shown in Figure 7. The data summarized in Table I reveal a reasonably good agreement between the two methods.

In an attempt to investigate the influence of the organization of myosin filaments into A bands on the low-affinity site

[2] Raising the KCl concentration from 80 to 140 mM to simulate the ionic strength effect of the highest concentration of divalent cations used (20 mM) had no effect on the digestion patterns.

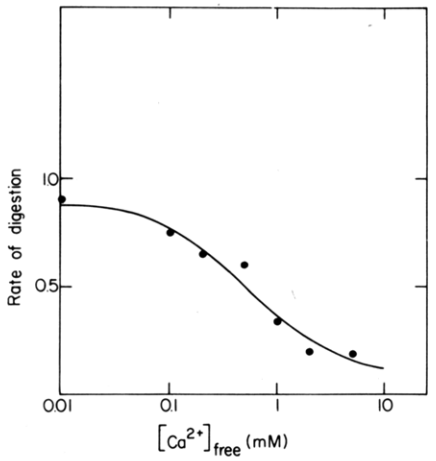

FIGURE 7: Titration of the low-affinity metal binding site of myofibrillar myosin (method II). Myofibrils (0.3 mg/mL) in 80 mM KCl–20 mM Tris-HCl, pH 8.5, were digested with 20 μg/mL chymotrypsin. The rates were normalized with respect to the rate obtained at 1 μM free Ca^{2+}.

digestibility, we have carried out the proteolysis of myosin filaments. The ionic conditions were identical with the ones of Figure 7. When the rate of digestion was assessed by following the rate of optical density decrease at 360 nm (method II), the digestion profile was S shaped with the midpoint corresponding to about 3 mM Mg^{2+}. When the digestion was followed by measuring the amount of myosin digested in a given time interval by $NaDodSO_4$–polyacrylamide gel electrophoresis (method I), the digestion profile showed progressive inhibition beginning at ca. 5 mM ion concentration, but no saturation could be seen even at 20 mM. When the amount of HMM was being measured, the profile showed progressive inhibition of production of 150 000- and 130 000-dalton chains of HMM, but a new band lying between these two bands appeared concomitantly, giving rise to the increase in the total intensity of the bands in the HMM region.

Time Course of Subfragment Formation. Two features of the digestion profiles of Figure 2 require further clarification. The first feature is the apparent allosteric-like inhibition of the chymotryptic attack at the HMM junction clearly visible in Figure 2, where at low Mg^{2+} concentration only S-1 is produced (as if the HMM junction were protected). The second feature is the incomplete inhibition of S-1 formation at higher than saturating Mg^{2+} concentrations. In order to clarify these points, we have followed the time course of digestion of myofibrils below and above the K_d for Mg^{2+}. Figure 8 (inset) shows the digestion products of myofibrillar myosin at different times during proteolysis in the presence of a low divalent cation concentration. The gels were scanned, and the intensity corresponding to myosin, HMM, and S-1 was plotted as a function of time in Figure 8. It is seen that both S-1 and HMM are produced at the outset and that eventually all HMM is converted into S-1. It follows that the observed rate of S-1 production is an overstimation of a true rate at which S-1 is created from myosin.

Figure 9 shows the time course of subfragment production under conditions at which the Nbs_2 light chains are fully saturated with Mg^{2+}. As expected, the rate of production of S-1 is much smaller than the rate of production of HMM. However, a decline in the amount of HMM produced at later times occurs concomitantly with an increase in the amount of S-1, which is formed even above the Mg^{2+} concentration where the Nbs_2 light chains of myofibrillar myosin are nearly fully saturated. Most likely, this S-1 is produced from soluble HMM which has a lower association constant for Mg^{2+} at the

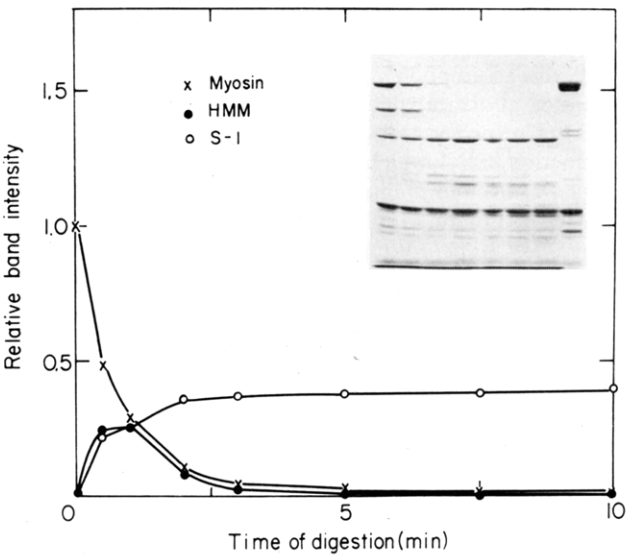

FIGURE 8: Time course of digestion of myofibrillar myosin in the presence of 0.05 μM free Mg^{2+}. Myofibrils (1.6 mg/mL) were in 80 mM KCl–20 and mM Tris-HCl, pH 8.5. Chymotrypsin (180 μg/mL) was added at time zero and the reaction stopped by the addition of 1 mM PMSF at the times indicated. The inset shows $NaDodSO_4$–polyacrylamide gel electrophoresis of the myofibrillar digest after (from left to right) 0.5, 1, 2, 3, 5, 7.5 and 10 min. The first gel at the right of the inset shows intact myofibrils. The curves were obtained by monitoring the band intensity of the heavy chains of myosin, HMM, and S-1. The peaks were normalized with respect to the amount of actin and expressed as the fraction of the myosin peak at time zero: (×) myosin; (●) HMM; (○) S-1.

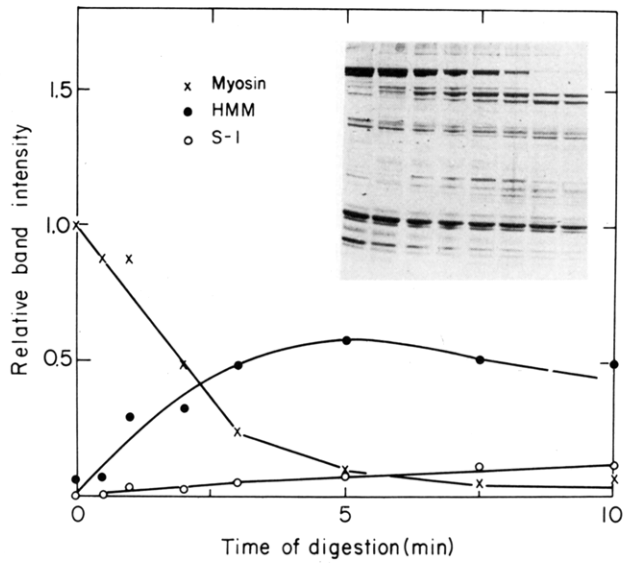

FIGURE 9: Time course of digestion of myofibrillar myosin in the presence of 10 μM free Mg^{2+}. The conditions are as described in Figure 8. The inset shows $NaDodSO_4$–polyacrylamide gel electrophoresis of the myofibrillar digest after (from left to right) 0, 0.5, 1, 2, 3, 5, 7.5, and 10 min of digestion. The curves were obtained as described in Figure 8.

high-affinity metal binding site than myofibrillar myosin (see Discussion). Below we correct for this effect to compute the true metal ion binding profile.

Discussion

The use of a digestion technique for the determination of divalent cation binding curves and the in vivo affinity constants rests on the assumption that the fractional saturation of the binding site results in the proportional inhibition of proteolysis at this site. The use of method I ($NaDodSO_4$–polyacrylamide gel electrophoresis) for detection of the digestion products

further assumes that S-1 is formed only from the myosin filaments arranged in the A bands. As shown in Figures 8 and 9, this assumption is incorrect: both S-1 and HMM are generated at a rate which depends on Mg^{2+} concentration. HMM then further decays to S-1. It is necessary to estimate the fraction of S-1 which has been produced by digestion of soluble HMM and to introduce an appropriate correction to the data of Figure 2. This is attempted below.

Digestion Model. We have considered the following simple model of chymotryptic digestion of myofibrillar myosin:

$$\text{Myo} \xrightarrow{k_1} \text{S-1} + \text{1h-Myo}$$

$$\text{1h-Myo} \xrightarrow{k_1} \text{S-1} + \text{rod}$$

$$\text{HMM} \xrightarrow{k_2} \text{S-1} + \text{1h-HMM}$$

$$\text{1h-HMM} \xrightarrow{k_2} \text{S-1} + \text{2S-2}$$

$$\text{Myo} \xrightarrow{k_3} \text{HMM} + \text{LMM}$$

where Myo is myosin and 1h-Myo and 1h-HMM are single-headed myosin and single-headed HMM, respectively. The differential equations describing the above five parallel processes were numerically integrated by using different sets of the rate constants k_1, k_2, and k_3. The best fit to the experimental data of Figure 8 was first determined by the least-squares method. However, there were many possible fits giving the same rms deviation from the data. For example, it was possible to match S-1 and myosin curves very closely at the expense of the HMM curve. Eventually the best set of rate constants was chosen from among all possible fits by inspection, requiring an equally good fit to each curve independently. The resulting fit was obtained with the following values for the rate constants: 0.9, 2.0, and 1.9 s^{-1} for k_1, k_2, and k_3, respectively.

It is interesting to point out that the rate of production of HMM at low Mg^{2+} concentration is of the same order of magnitude as the rate of production of S-1. This is in contrast to the digestion of myosin in vitro, where in the absence of divalent cations no HMM is produced (Weeds & Pope, 1977). The reason for this effect must be that at pH 8.5 the HMM junction is exposed to chymotryptic attack. Indeed, Ueno & Harrington (1981) showed that the rate of attack at the HMM junction increases sharply with pH. Also, Oda et al. (1980) suggested that actin can afford protection of the Nbs_2 light chains even in the absence of divalent cations. Thus, in myofibrils, chymotrypsin will preferably attack the unprotected HMM junction.

The best fit to the data characterizing myosin digestion at higher Mg^{2+} concentrations was obtained by a procedure analogous to the one described above. The rate constants for S-1 production from myosin (k_1), from HMM (k_2), and for HMM production (k_3) were 0.11, 0.09, and 1.0 s^{-1}, respectively. As expected, saturation of the Nbs_2 light chains' site caused a decrease in the rate of S-1 production by an order of magnitude, whereas the formation rate of HMM was hardly affected.

High-Affinity Binding. With the aid of the rate constants, it is now possible to correct for S-1 generation through HMM digestion. The computed time course of myofibrillar myosin digestion at low Mg^{2+} concentrations (0.05 μM), assuming S-1 is produced only from myosin, yields the HMM band which after 10 min of digestion is 3.5 times more intense than the S-1 band. At higher Mg^{2+} concentrations (10 μM), HMM is produced at a relatively faster rate and after 10 min gives rise to a band which is 23% stronger than the HMM band at low Mg^{2+} concentrations. The computation also shows that the S-1 band intensity at low Mg^{2+} concentrations should be 5 times more intense than at higher Mg^{2+} concentrations. The complete corrected HMM formation profile, therefore, looks as follows: Let the amount of HMM produced at low Mg^{2+} concentration be normalized to 1. Then at higher Mg^{2+} concentration, the amount of HMM is 1.23, the amount of S-1 at low Mg^{2+} concentration is 0.28, and the amount of S-1 at higher Mg^{2+} concentration is 0.057.

The corrected in vivo binding profile indicated that the apparent allosteric inhibition of the proteolysis at the HMM junction at low Mg^{2+} concentrations is illusory. The amount of HMM produced does not suddenly become zero below the metal ion concentration equal to the dissociation constant for the high-affinity site (K_d). It does increase a little above K_d because now there is no competition from S-1 formation. The Mg^{2+} binding constant estimated from the corrected profile differs little from the uncorrected constant estimated directly from Figure 2.

The second method for determination of metal binding to the high-affinity sites rests on the assumption that the rate of myofibril solubilization is proportional to the rate of the chymotryptic attack at the S-1 site. The kinetic analysis reveals that this assumption is incorrect because at metal ion concentrations both below and above the K_d for the high-affinity site HMM is produced as well. Thus, at each cation concentration, the rate of solubilization is higher than it would have been had HMM not been produced. This leads to an overestimation of the K_a by method II. For this reason, we believe that method I gives a more reliable estimate of the association constants for the high-affinity site.

Many values have appeared in the literature for the binding constants of Mg^{2+} and Ca^{2+} to myosin in solution. The values for Mg^{2+} range from 7.5×10^4 to 1.6×10^7 M^{-1} and those for Ca^{2+} from 1.4×10^5 to 2.8×10^8 M^{-1}. However, we will compare our results only with values obtained by a digestion method. Thus, our values for Mg^{2+} seem to be 1 order of magnitude higher than those obtained by Weeds & Pope (1977) and Kardami et al. (1980) for myosin in solution. On the other hand, our binding constant value for Ca^{2+} to myosin in vivo seems to be identical with the values of those authors. Thus, it seems that when going from isolated light chains to myosin in solution and then to myosin in vivo, the binding constant for Mg^{2+} increases first by 2 orders of magnitude and then by an additional order of magnitude, whereas in the case of Ca^{2+} the total increase is only by 1 order of magnitude.

Low-Affinity Binding. The digestion profiles at higher divalent metal concentrations showed that HMM was the predominant proteolytic product. The residual S-1 which has been found after long digestion times (Figure 9) was most likely produced from soluble HMM. The amount produced was so small, however, that it was unnecessary to correct for this effect. This argues in favor of the explanation that under our experimental conditions the HMM junction is exposed to the chymotryptic attack. The fact that divalent cations regulate the rate of this attack and that this regulation is not due to an ionic strength effect[2] seems to indicate the presence of one or more divalent metal binding sites at, or in the vicinity of, the HMM junction.

There are three possible ways in which the low-affinity site could be distributed at or near the HMM junction: (1) There could be one low-affinity site at each of the two heavy chains of myosin. (2) One heavy chain could have a low-affinity site (L) and the other a high-affinity site (H). (3) One heavy chain could have a low-affinity site L and the other a cation binding affinity even smaller than that of the L site or it could be

altogether insensitive to divalent cations. The fact that when the divalent metal ion concentration increases from below to above K_d for the high-affinity site there is no concomitant decrease in the amount of HMM produced argues against the second possibility. (The curve fitting to the kinetic data suggest that k_3 decreased by a factor of 2 when Mg^{2+} concentration was increased from 0.05 to 10 μM, but such variation is within the limits of error for the curve-fitting procedure.) It is more difficult to decide whether HMM junctions on both subunits of myosin are sensitive to metal ion binding. Figure 6 shows that even at 20 mM Ca^{2+} some HMM is being produced. A careful inspection of Figure 5 reveals, however, that at high Ca^{2+} concentrations a new band migrating between 150K- and 130K-dalton HMM bands appears. The intensity of the old HMM bands decreases sharply at high Ca^{2+} concentrations, but the total intensity of bands migrating between 150K and 130K decreases little as a result of the appearance of this new band. The same is true of HMM bands in the myosin digestion patterns. It thus appears that high divalent cation concentrations block the old proteolytic site but that at the same time a new site becomes susceptible to attack. The digestibility of myosin as a function of metal ion concentration presents a much more clear picture: there is a clear inflection in the digestibility profiles around 1–2 mM. A similar result is obtained for purified myosin. Table I quotes estimates of K_a obtained from the myosin digestion profiles.

The binding constant for Ca^{2+} and Mg^{2+} for the low-affinity site obtained by method II is close to the constant estimated by method I, which is in agreement with our observation that when the S-1 junction is blocked by the divalent cation the rate of myofibril solubilization equals the rate of HMM formation.

Morimoto & Harrington (1974) have demonstrated that there exists in myosin a class of low-affinity binding sites for Ca^{2+} with the binding constant of the order of 10^4 M^{-1}. If the sites reported here coincide with the ones observed by Morimoto and Harrington, then the difference in affinity may be due either to pH or to the fact that in our experiments myosin formed a part of the organized structure of the sarcomere.

Acknowledgments

We thank Rina Levy for excellent technical assistance.

References

Alexis, N., & Gratzer, W. B. (1978) *Biochemistry 17*, 2319–2325.

Bagshaw, C. R. (1977) *Biochemistry 16*, 59–67.

Bagshaw, C. R., & Kendrick-Jones, J. (1979) *J. Mol. Biol. 130*, 317–336.

Bálint, M., Shaefer, A., Birő, N. A., Menczel, L., & Fejer, E. (1971) *Physiol. Chem. Phys. 3*, 455–466.

Beinfeld, M. G., Bryce, D. A., Kochavy, D., & Martonosi, A. (1975) *J. Biol. Chem. 250*, 6282–6287.

Borejdo, J., & Oplatka, A. (1981) *Nature (London) 291*, 322–323.

Fabiato, A., & Fabiato, F. (1979) *J. Physiol. (Paris) 75*, 463–505.

Garamvölgyi, N. (1968) in *Symposium on Muscle* (Ernst, E., & Straub, F. B., Eds.) pp 114–119, Akademiai Kiado, Budapest.

Highsmith, S., Kretzchmar, M., O'Konski, C. T., & Morales, M. F. (1977) *Proc. Natl. Acad. Sci. U.S.A. 74*, 4986–4990.

Holroyde, M. J., Potter, J. D., & Solaro, R. J. (1979) *J. Biol. Chem. 254*, 6478–6482.

Huxley, H. E. (1969) *Science (Washington, D.C.) 164*, 1356–1358.

Kardami, E., Alexis, M., de la Paz, P., & Gratzer, W. (1980) *Eur. J. Biochem. 110*, 153–160.

Laemmli, U. K. (1970) *Nature (London) 227*, 680–685.

Lehman, W., & Szent-Györgyi, A. G. (1975) *J. Gen. Physiol. 66*, 1–30.

Mendelson, R. A., & Cheung, P. (1976) *Science (Washington, D.C.) 194*, 190–192.

Morimoto, K., & Harrington, W. F. (1974) *J. Mol. Biol. 88*, 693–709.

Oda, S., Oriol-Audit, C., & Reisler, E. (1980) *Biochemistry 19*, 5614–5618.

Stromer, M. H., Goll, D. E., & Roth, L. F. (1967) *J. Cell. Biol. 34*, 431–445.

Sugden, E. A., & Nihei, T. (1969) *Biochem. J. 113*, 821–827.

Sutoh, K., & Harrington, W. F. (1977) *Biochemistry 16*, 2441–2449.

Ueno, H., & Harrington, W. F. (1981) *J. Mol. Biol. 149*, 619–640.

Watterson, J. G., Kohler, L., & Schaub, M. C. (1979) *J. Biol. Chem. 254*, 6470–6477.

Weeds, A. G., & Pope, B. (1977) *J. Mol. Biol. 111*, 129–157.

Werber, M. M. (1978) *Experienta 34*, 575–576.

Werber, M. M., Gaffin, S. L., & Oplatka, A. (1972) *J. Mechanochem. Cell Motil. 1*, 91–96.

Werber, M. M., Szent-Gyorgyi, A. G., & Fasman, G. D. (1973) *J. Mechanochem. Cell Motil. 2*, 35–43.